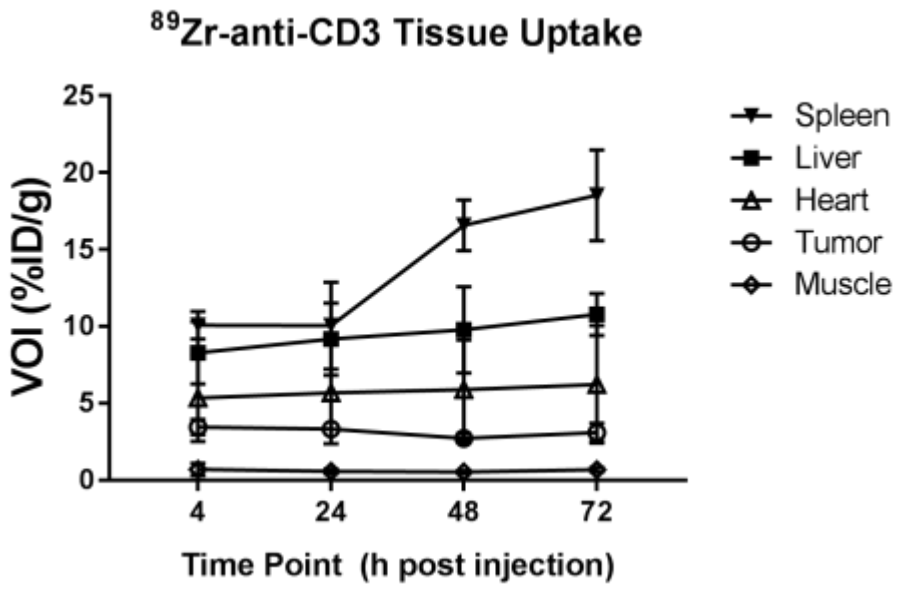
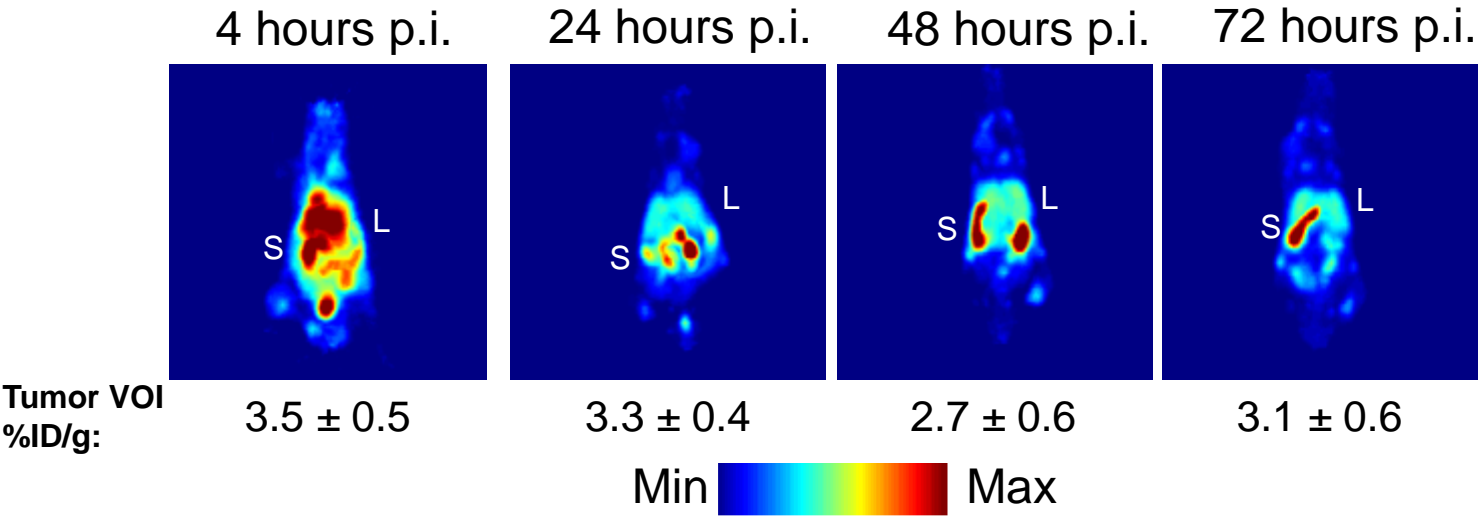


**Supplementary Figure 1. Time course imaging of <sup>89</sup>Zr-anti-IFN $\gamma$ .** Mice were injected with <sup>89</sup>Zr-anti-IFN $\gamma$  and images of MIP are shown for each time point (top). L = liver, S = spleen. A plot of the volumes-of-interest obtained from select tissues is shown over time from 24-120 h p.i.



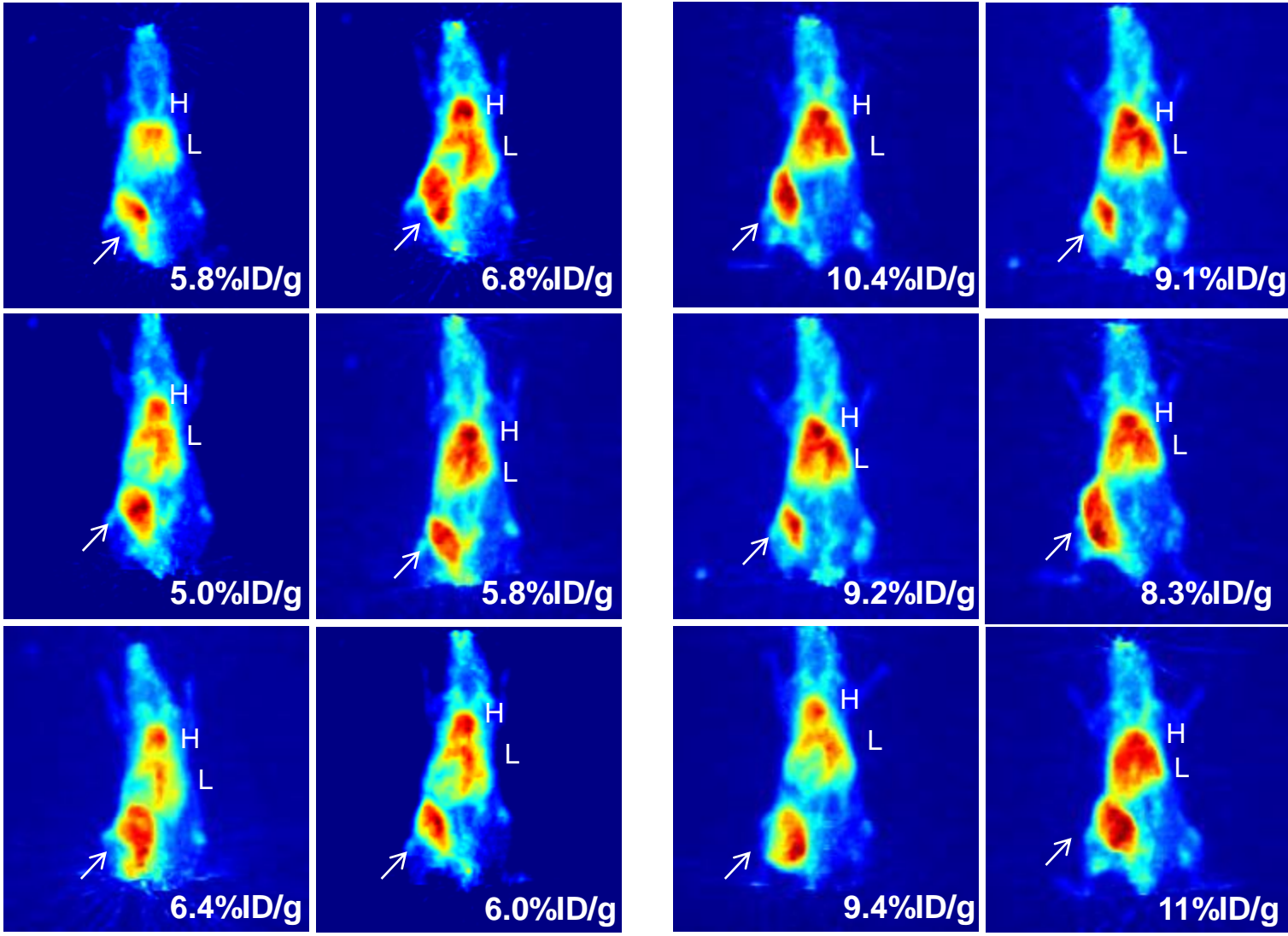
**Supplementary Figure 2. Time course imaging of <sup>89</sup>Zr-anti-CD3.** Mice were injected with <sup>89</sup>Zr-anti-CD3 and images of MIP are shown for each time point (top). L = liver, S = spleen. A plot of the volumes-of-interest obtained from select tissues is shown over time from 4-72 h p.i.

<sup>89</sup>Zr-anti-IFN $\gamma$  PET in TUBO-bearing BALB/c

A

Control

Vx



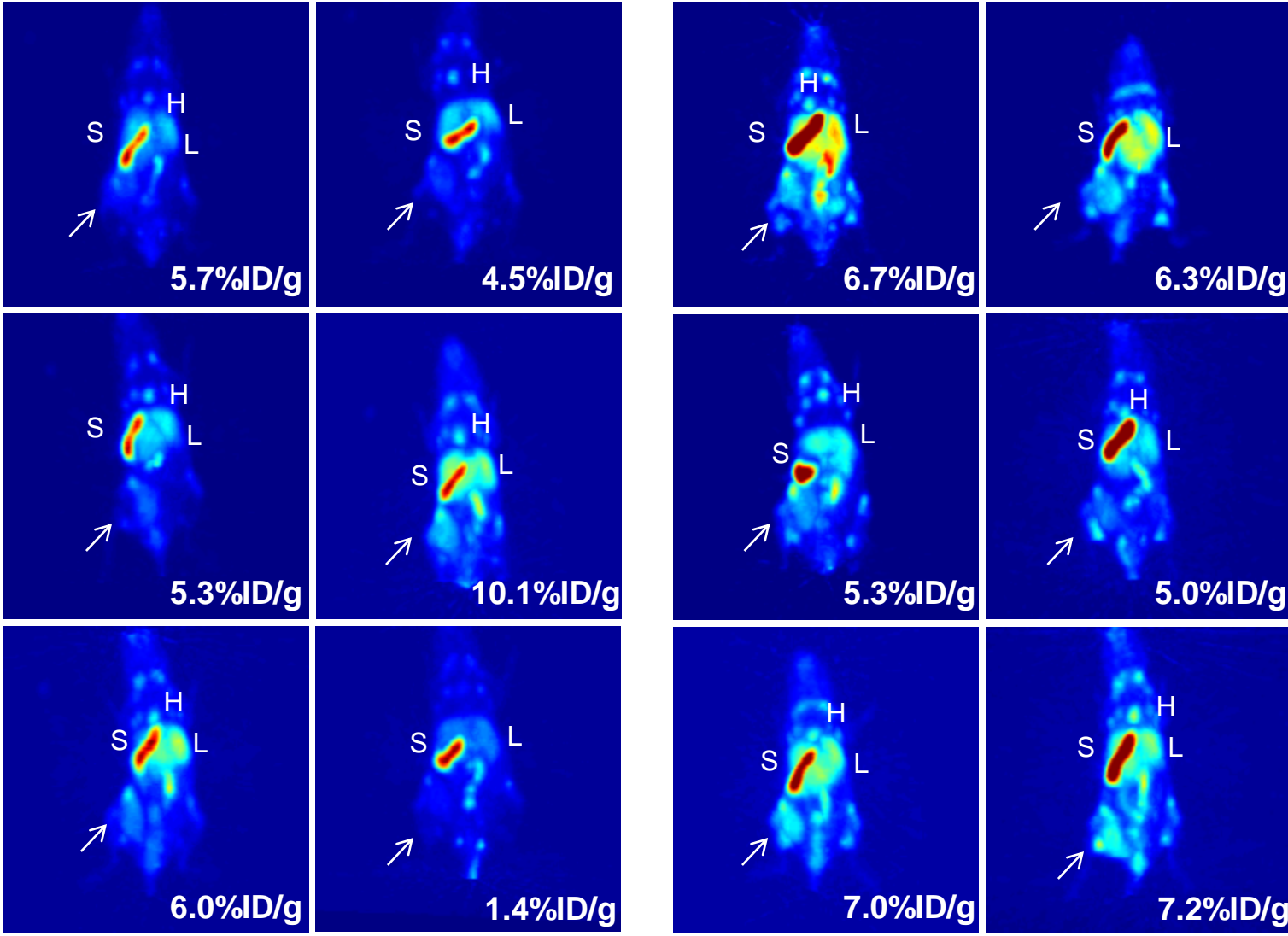
Min  Max

<sup>89</sup>Zr-CD3 PET in TUBO-bearing BALB/c

B

Control

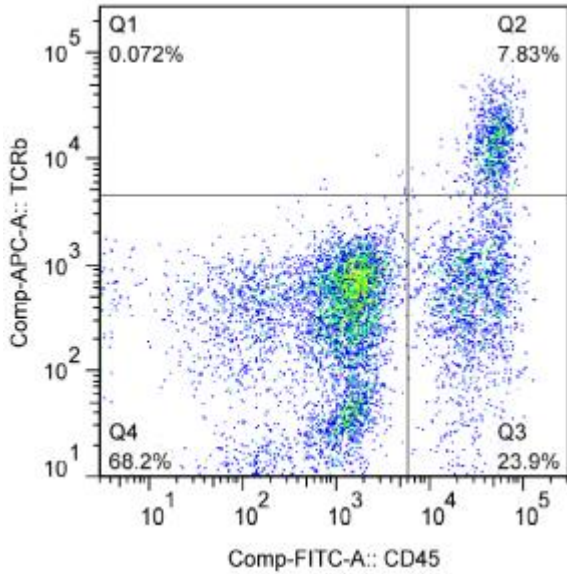
Vx



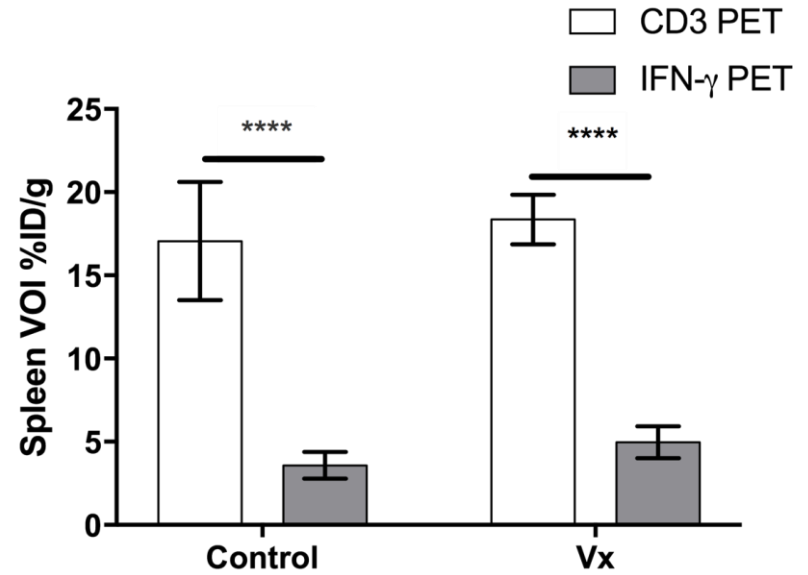
Min Max

**Supp. Fig 3.** MIP images of (A) <sup>89</sup>Zr-anti-IFN $\gamma$  and (B) <sup>89</sup>Zr-anti-CD3 detection in all control (left) and vaccinated (right) TUBO bearing mice.

**A** T cell infiltration in TUBO tumors

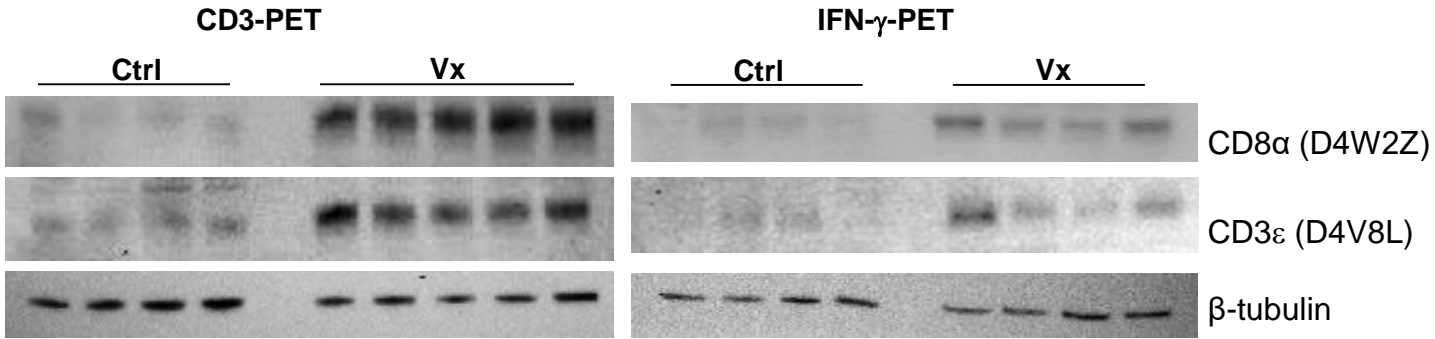


**B**



**Supplementary Figure 4. T cell detection in TUBO-bearing BALB/c.** A) Tumors from untreated TUBO-bearing mice were dissociated and stained with CD45, to detect total leukocyte infiltrates, and the T cell receptor beta chain (TCR $\beta$ ), to identify the T cell fraction, by flow cytometry. B) Spleen VOIs were calculated for each TUBO-bearing mouse imaged with either <sup>89</sup>Zr-anti-IFN $\gamma$  or <sup>89</sup>Zr-anti-CD3.

C

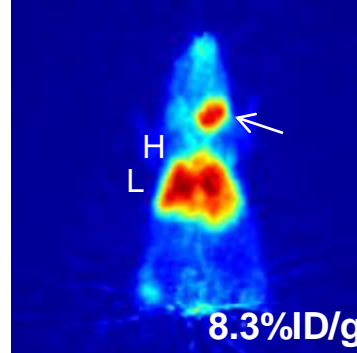
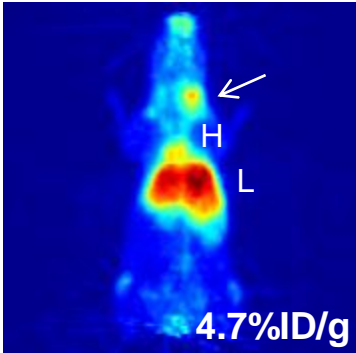
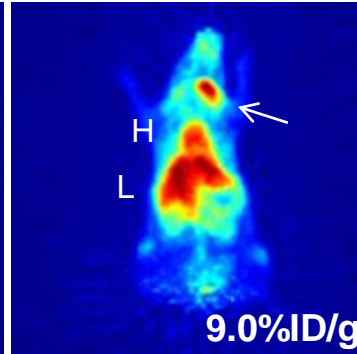
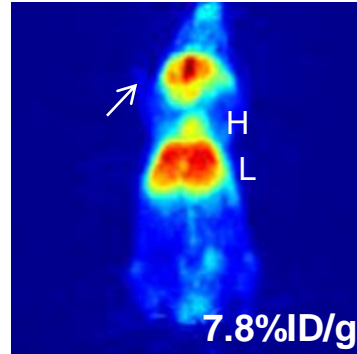
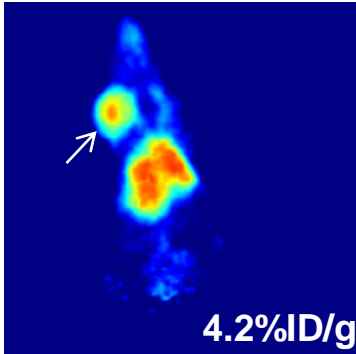
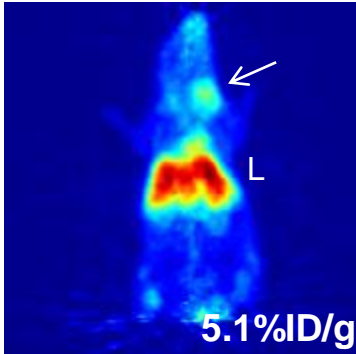


**Supplementary Figure 5. Immunoblot detection of T cell markers in imaged TUBO-bearing mice.** Western blots from lysed decayed tumor tissues post-CD3 or IFN- $\gamma$  PET were conducted to analyze presence of CD3 and CD8 protein in the Vx vs Ctrl mice.

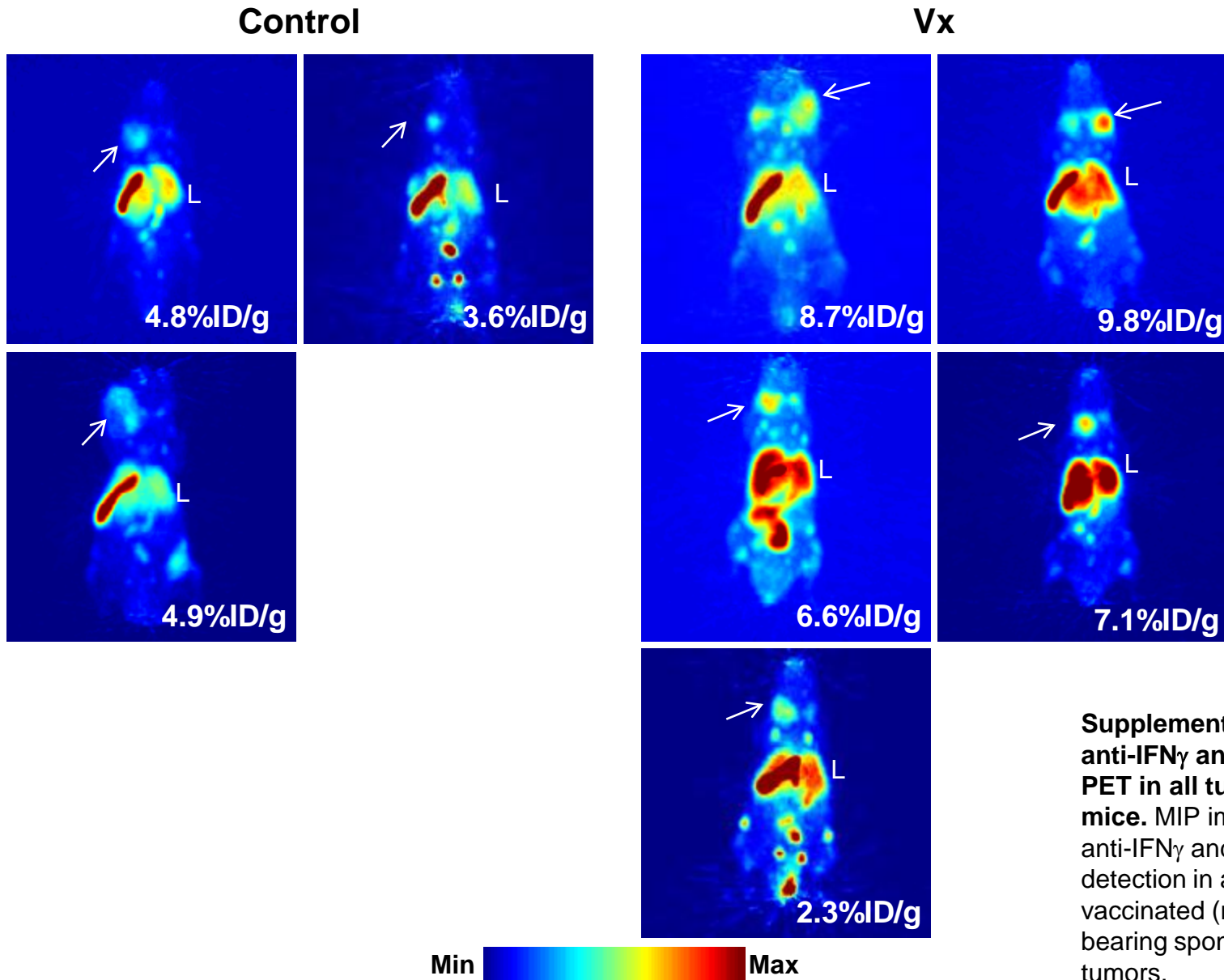
**A**  $^{89}\text{Zr}$ -IFN $\gamma$  PET in NeuT

**Control**

**Vx**

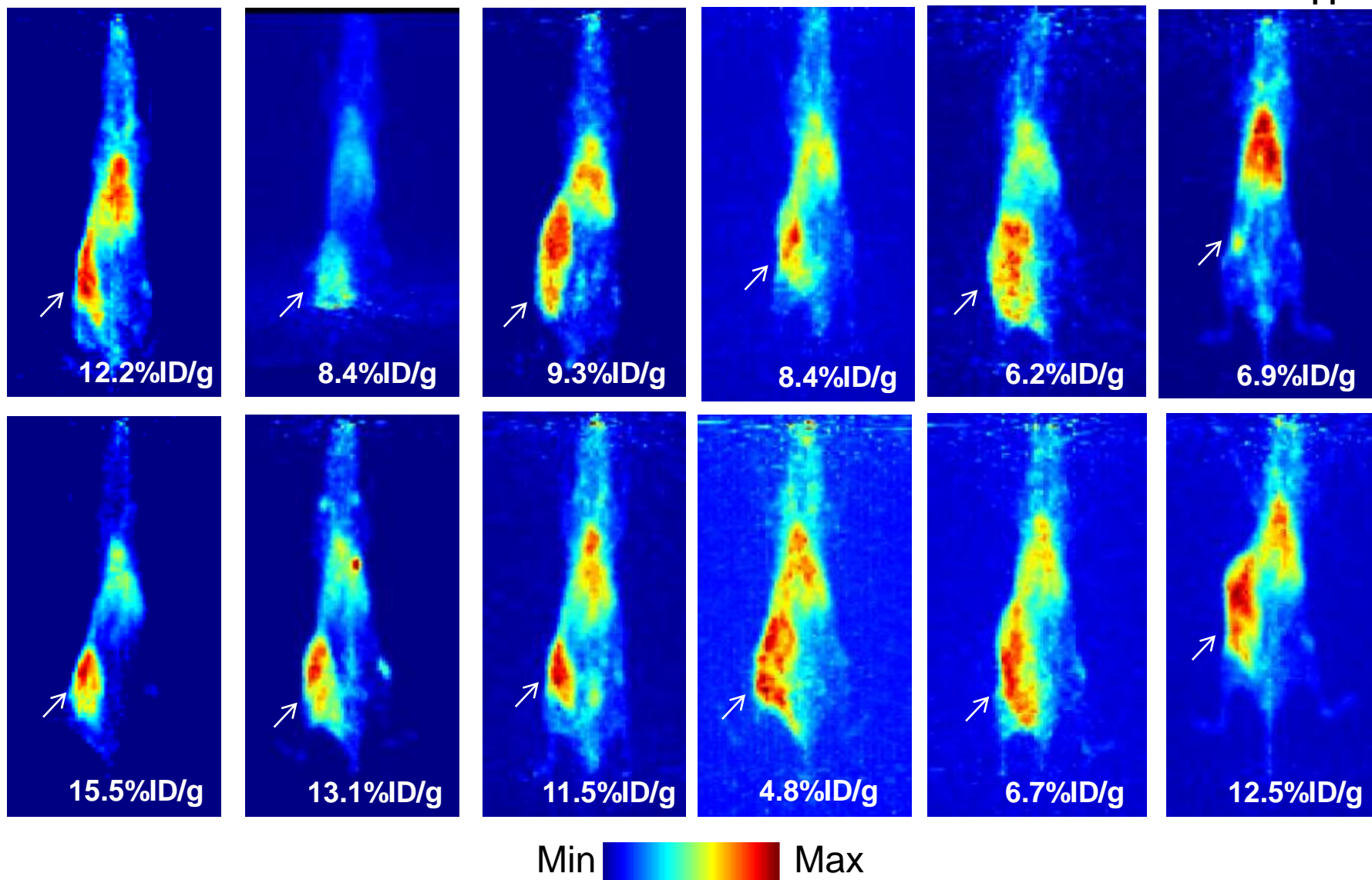


**B**  $^{89}\text{Zr}$ -CD3 PET in NeuT



**Supplementary Figure 6.**  $^{89}\text{Zr}$ -anti-IFN $\gamma$  and  $^{89}\text{Zr}$ -anti-CD3 PET in all tumor-bearing NeuT mice. MIP images of (A)  $^{89}\text{Zr}$ -anti-IFN $\gamma$  and (B)  $^{89}\text{Zr}$ -anti-CD3 detection in all control (left) and vaccinated (right) NeuT mice bearing spontaneous salivary tumors.



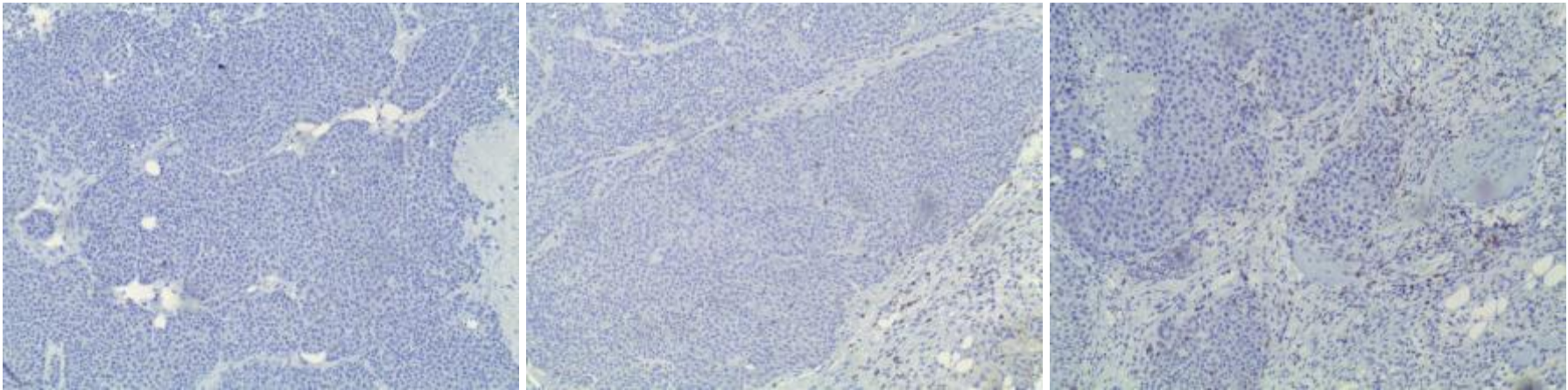


**Supplementary Figure 7.**  $^{89}\text{Zr}$ -IFN- $\gamma$  PET of vaccinated mice for correlation to tumor growth. MIP images of  $^{89}\text{Zr}$ -anti-IFN $\gamma$  detection in all vaccinated TUBO mice bearing tumors.

Ctrl

7.16.4

Vx



**Supplementary Figure 8. CD8 IHC after ITx.** Intratumoral localization of CD8 was analyzed by IHC on FFPE tissue (100x)